IEEE Access
Multidisciplinary | Rapid Review | Open Access Journal

Received September 17, 2018, accepted October 4, 2018, date of publication October 10, 2018, date of current version October 29, 2018.

Digital Object Identifier 10.1109/ACCESS.2018.2875029

Dual-Band Circularly Polarized Antenna With Wide Axial Ratio Beamwidths for Upper Hemispherical Coverage

YU-XIANG SUN, KWOK WA LEUNG, (Fellow, IEEE), AND JIAN REN
The State Key Laboratory of Millimeter Waves, Department of Electronic Engineering, City University of Hong Kong, Hong Kong
The Information and Communication Technology Centre, CityU Shenzhen Research Institute, Shenzhen 518057, China

Corresponding author: Jian Ren (renjian.ee@my.cityu.edu.hk)

This work was supported in part by the Fundamental Research Program of Shenzhen City under Grant JCYJ20170818094814530 and in part by the Joint Research Fund for Overseas Chinese, Hong Kong and Macao Scientists of the National Natural Science Foundation of China under Project 61728106.

ABSTRACT This paper presents a dual-band circularly polarized cross-dipole antenna with wide axial ratio beamwidths for full upper hemispherical coverage for GPS L1 and L2 bands. The antenna has curved radiating arms and a corrugated back cavity to enhance the beamwidth. A wideband hybrid coupler is used to feed the antenna at the two nearby frequency bands. Experimental results show that very wide 3-dB AR beamwidths of over 200° can be obtained, fully covering the upper hemisphere for the two GPS bands.

INDEX TERMS Broadbeam antenna, cross-dipole antenna, circular polarization, dual-band antenna, GPS antenna.

I. INTRODUCTION

The global positioning system (GPS) has been widely deployed in military, commercial, and civilian applications [1], [2]. The circular polarization (CP) is used in this system because they can suppress the multipath fading problem. Also, as compared with the linearly polarized antenna, the CP antenna are less sensitive to the angle between the transmitting and receiving antennas [3], [4]. For GPS systems, to obtain higher precision, it is useful for antennas to have broad AR beamwidths that can cover the upper hemisphere to effectively receive low-elevation satellite signals. Different frequency bands are used in various GPS applications [5]. Two of them, L1 (1.575 GHz) and L2 bands (1.227 GHz), are commonly used by satellites and it is therefore desirable to include them in GPS antenna designs.

Traditionally, quadrifilar helix antennas (QHA) with cardioid-shaped radiation patterns and broad gain beamwidths have been used for GPS applications [6]–[9]. However, it is inconvenient to fabricate their curl arms and the fabrication tolerance can affect the antenna performance significantly. Furthermore, more than one QHA are normally needed [10], [11] for a dual-band design, increasing the complexity of the antenna structure.

In recent years, planar cross-dipole antennas have been reported for wideband [12]–[16] and dual-/multi-band CP applications [17]–[19]. By taking advantage of the inherent phase difference between the signal line and ground plane [20],]21], the sequential rotation feed network can be simplified considerably. Also, the artificial magnetic conductor [14], [17] or high impedance surface [18] can be incorporated into the antenna structures to reduce the antenna profile or enhance the front-to-back ratio. However, their AR beamwidths are generally insufficient to fully cover the upper hemisphere. Although the CP designs in [22]–]24] can cover the upper hemisphere, they are for single-band applications only. In [24], it uses two antenna ports to achieve hemispherical coverage, complicating the configuration.

In this paper, a dual-band CP cross-dipole antenna with wide AR beamwidth that fully cover the upper hemisphere is investigated. The antenna has unequal dipole-arm lengths to obtain two operating bands. A very wide CP beamwidth of more than 200° is achieved by using curved dipole arms and a corrugated cavity. The antenna is simulated using ANSYS HFSS. For demonstration, a prototype was fabricated and measured in GPS L1 and L2 bands, and reasonable agreement between the measured and simulated results is obtained.

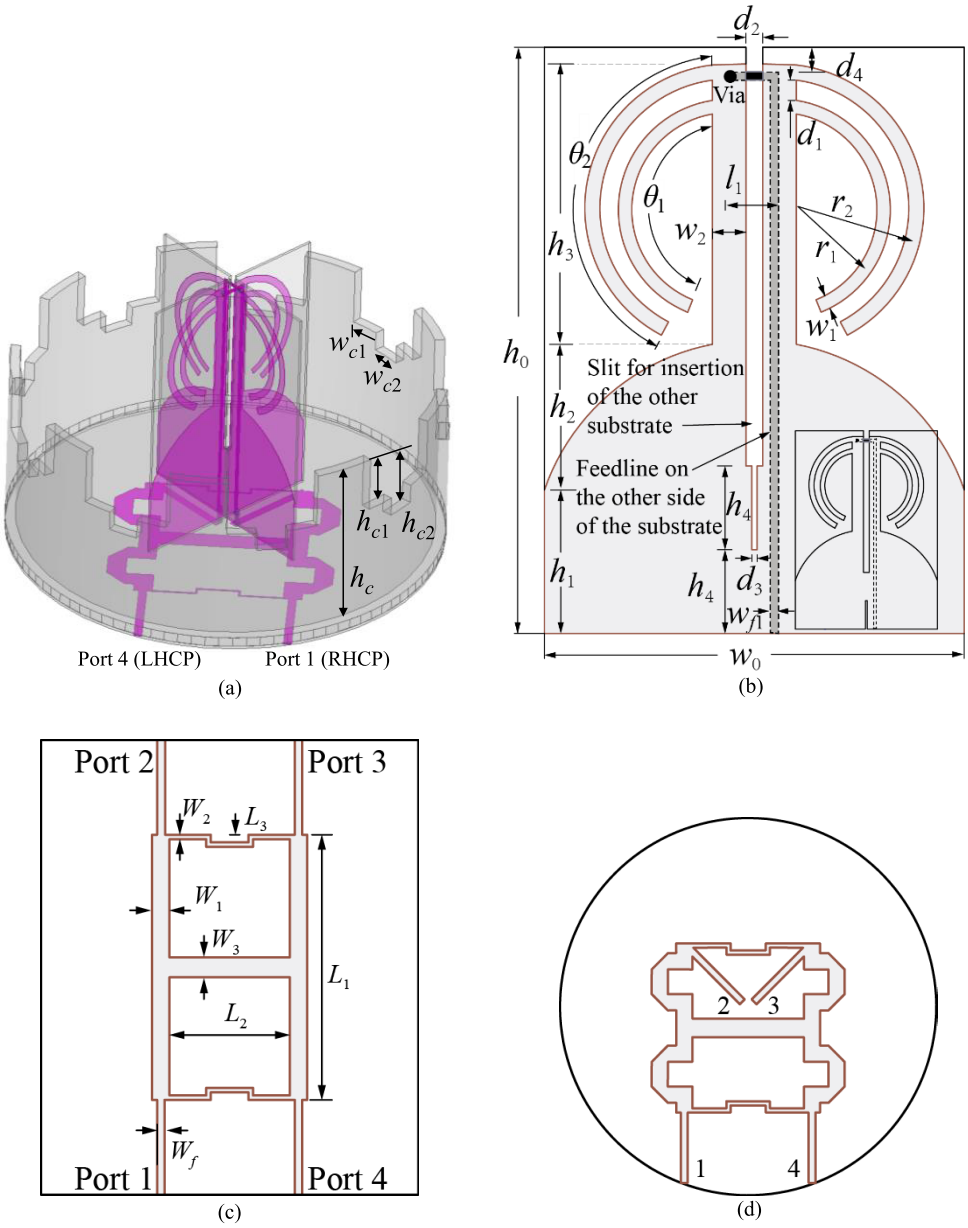

FIGURE 1. Configuration of dual-band CP antenna. (a) Perspective view of the whole design. (b) Layout of one of two substrates. The inset shows the layout of the other substrate. (c) Bottom view of the original wideband cascaded hybrid coupler. (d) Folded version of (c).

II. ANTENNA CONFIGURATION

Fig. 1(a) shows the configuration of the dual-band CP antenna that consists of a cross-dipole printed on two perpendicular substrates, a circular aluminum back cavity, and a feed network with a cascaded hybrid coupler. The cross-dipole has unequal curved arms, and each arm has a uniform width of w_1. For the smaller curved dipole arm, its radius and subtended angle are denoted by r_1 and θ_1, respectively, whereas the corresponding parameters of the larger dipole are r_2 and θ_2. The cross dipoles are placed inside the cavity, and beneath the cavity is the feed network. A via passing through the cavity is used to connect the cross-dipole to the feed network. The circular cavity has a radius of R, height of h_c, and thickness of t_c. A non-uniform corrugation is introduced to the cavity side wall to broaden the beamwidth. As shown in Fig. 1(b), the cross dipole and ground plane are printed on one side of each substrate, whereas a 50-Ω microstrip feedline is printed on the other side of the substrate. Each substrate has a size of $h_0 \times w_0$, dielectric constant of ε_r, thickness of t, and a slit for the perpendicular insertion of the other substrate. After the mutual insertion of the two substrates, a short adhesive conducting tape of length l_1 is stuck across the slit, connecting the microstrip feedline to the dipole ground through a via. It forms a merchant balun [25]

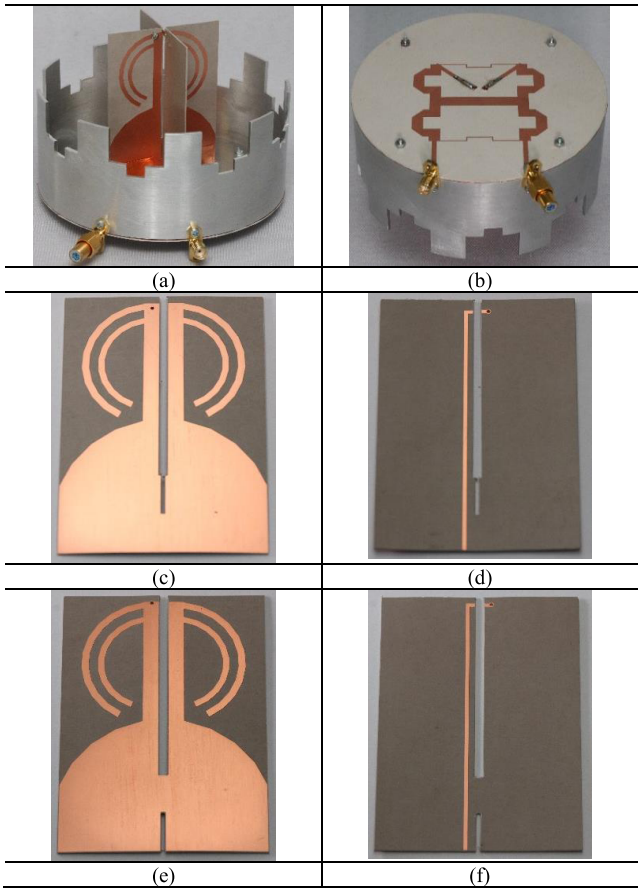

FIGURE 2. Prototype of dual-band CP antenna. (a) Perspective view of the whole antenna. (b) Feed network mounted beneath back cavity. (c) Printed curved arms and ground. (d) Microstrip feedline printed on the other side of the substrate. (e) Curved arms and ground printed on the second substrate. (f) Microstrip feedline printed on the other side of second substrate.

to obtain a differential feed for the dipole. The inset shows the other substrate. Basically, the layout is the same as that of the first substrate, but the narrow slit is now fabricated at the bottom. Also, the horizontal conducting strip is slightly shifted upwards to avoid shorting that of the first substrate.

L1 band (1.227 GHz) is nearby L2 band (1.575 GHz). Since the frequency ratio of these two bands is small, it will require very narrow coupled lines for a dual-band hybrid coupler. Therefore, a wideband two-stage cascaded hybrid coupler [26] is used here. Fig. 1(c) shows the original design of the two-stage hybrid coupler, whereas Fig. 1(d) shows the folded version for moving the feed points (Ports 2 and 3 in Fig. 1(d)) to near the center. The feed substrate has a dielectric constant of ε_{r1} and thickness of t_1. Its radius is the same as that of the cavity.

III. SIMULATED AND MEASURED RESULTS

To begin with, the wideband cascaded hybrid coupler was designed to cover the two bands. Table 1 lists its simulated phase difference and amplitude imbalance between the two output ports, along with the S-parameters of the four ports.

TABLE 1. Simulated performance of wideband feed network.

10-dB impedance bandwidth	1.08–1.82 GHz (51.0%)
90°±5° phase difference	1.00–1.86 GHz (60.1%)
1.5-dB amplitude imbalance	1.10–1.72 GHz (44.0%)
Overlapping bandwidth	1.10–1.72 GHz (44.0%)

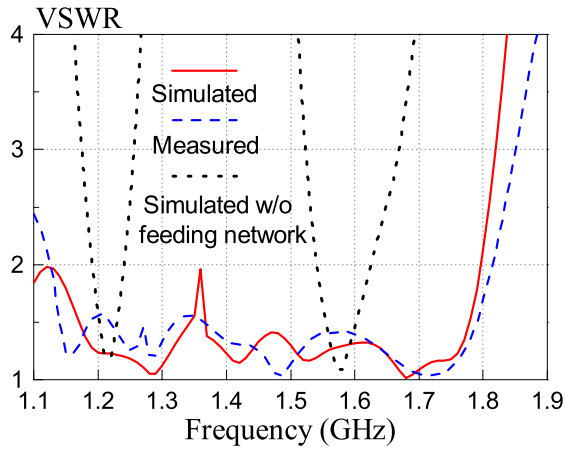

FIGURE 3. Measured and simulated VSWRs of dual-band CP antenna: $R = 53.75$ mm, $h_c = 45$ mm, $h_{c1} = 14.5$ mm, $h_{c2} = 19.5$ mm, $w_{c1} = 7.5$ mm, $w_{c2} = 7.5$ mm, $t_c = 1.5$ mm, $\varepsilon_r = 6.15$, $\varepsilon_{r1} = 2.94$, $t = 0.635$ mm, $t_1 = 0.76$ mm, $h_0 = 70$ mm,$h_1 = 17.14$ mm, $h_2 = 17.38$ mm, $h_3 = 33.48$ mm, $h_4 = 10$ mm, $d_1 = 2.42$ mm, $d_2 = 2$ mm, $d_3 = 0.635$ mm, $d_4 = 3$ mm, $r_1 = 12.4$ mm, $r_2 = 16.3$ mm, $\theta_1 = 158$ deg, $\theta_2 = 152$ deg, $w_0 = 50$ mm,$w_1 = 1.8$ mm, $W_1 = 4.62$ mm, $W_2 = 0.45$ mm, $W_3 = 5.25$ mm, $l_1 = 6.94$ mm, $L_1 = 70$ mm, $L_2 = 31.88$ mm, $L_3 = 2$ mm, $W_f = 1.92$ mm, and $W_{f1} = 0.92$ mm.

The overlapping bandwidth is 44.0% (1.10–1.72 GHz), which is sufficient for GPS L1 and L2 bands.

Next, the antenna with the feed network was simulated and optimized. To verify the simulations, the antenna was fabricated and measured. Fig. 2 shows the different parts of the prototype including the cross dipoles. In our measurements, the voltage standing wave ratio (VSWR) was measured with the Keysight VNA 8361A, whereas the AR, radiation pattern, realized antenna gain, and total antenna efficiency were measured with a Satimo StarLab System. Since our antenna is designed for GPS applications, only the results of the right-handed CP (RHCP) port (Port 1) are presented here. Fig. 3(a) shows the measured and simulated VSWRs of the antenna, with reasonable agreement between them. With reference to the figure, the measured and simulated impedance bandwidths (VSWR ≤ 2) are 46.3% (1.13–1.81 GHz) and 47.8% (1.10–1.79 GHz), respectively. Fig. 3 also shows the simulated VSWR without the feed network. With reference to the figure, two frequency bands corresponding to L1 and L2 bands are found, showing that the wideband matching of the full structure is due to the feed network.

Fig. 4 shows the simulated current of the cross-dipole. With reference to the figure, the currents mainly flow along the outer and inner dipole arms at 1.227 GHz (L2 band) and 1.575 GHz (L1 band), respectively, which can be expected.

TABLE 2. Comparison between our design and some previous dual-band CP antennas.

Antenna	Ref. [10]		Ref. [17]		Our design	
Structure	Combine two quadrifilar helix antennas together		Single planar cross dipole on AMC surface		Single vertical cross dipole with cavity	
Overall size (λ_0^*)	$0.140\lambda_0 \times 0.140\lambda_0 \times 0.387\lambda_0$ @1.615 GHz		$0.576\lambda_0 \times 0.576\lambda_0 \times 0.088\lambda_0$ @2.4 GHz		$0.573\lambda_0 \times 0.573\lambda_0 \times 0.296\lambda_0$ @1.227 GHz	
Operating frequencies (GHz)	1.615	2.492	2.4	5.2	1.227	1.575
Impedance bandwidth	28%	39%	16.7%	11.5%	46.3%	
AR bandwidth	Not available	Not available	8.30%	5.77%	13.0%	30.2%
Peak gain (dBic)	< 1	< 1	5.1	6.2	4.39	5.06
HPBW# (Degree)	> 180°	> 180°	60°	82°	103°	111°
AR beamwidth (Degree)	~ 100°	~ 100°	< 120°	< 60°	202°	211°

*λ_0 is the wavelength in air at the lower operating frequency.
The lower value in the two principle planes is listed.

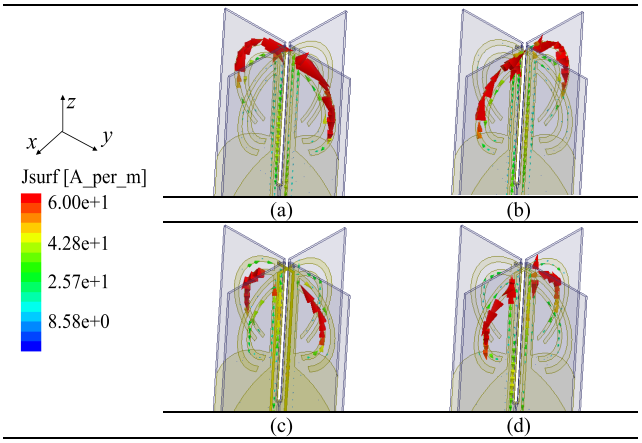

FIGURE 4. Simulated current distribution of dual-band CP antenna. (a) L2 band (1.227 GHz), $t = 0$. (b) L2 band, $t = T/4$. (c) L1 band (1.575 GHz), $t = 0$. (d) L1 band, $t = T/4$.

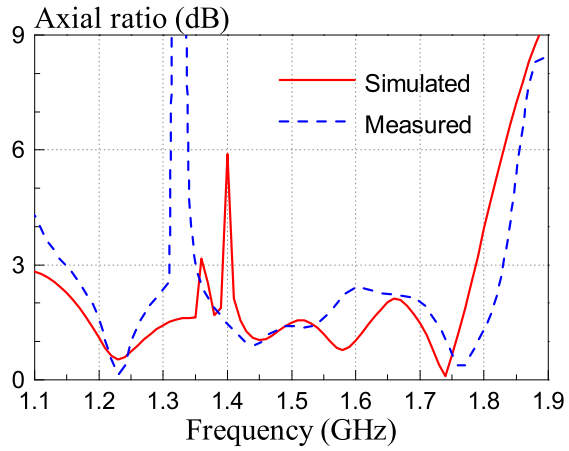

FIGURE 5. Measured and simulated ARs of dual-band CP antenna in boresight direction ($\theta = 0°$).

With reference to Fig. 4(a), the dipole currents at $t = 0$ mainly flow along the $+y$ direction in the *yoz*-plane, radiating the $+y$- directed E-field. In this case, the currents on all the other dipole arms are very weak. At $t = T/4$ (Fig. 4(b)),

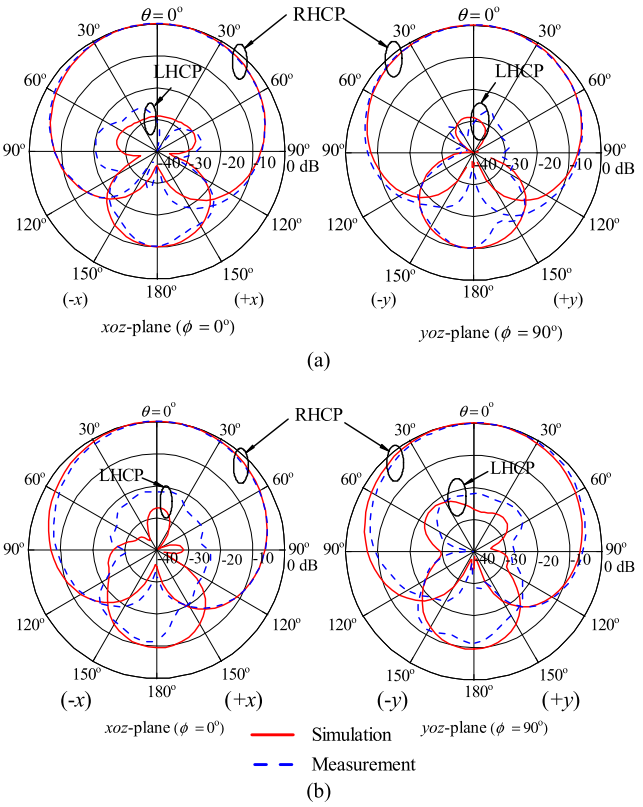

FIGURE 6. Measured and simulated radiation patterns of dual-band CP antenna in *xoz* ($\varphi = 0°$) and *yoz* planes ($\varphi = 90°$). (a) L2 band (1.227 GHz). (b) L1 band (1.575 GHz).

the currents mainly flow on the other pair of the outer arms in the $-x$ direction (*xoz*-plane). Therefore, the $-x$-directed E-field is radiated. As a result, RHCP fields can be generated at 1.227 GHz. Similar current variations at 1.575 GHz (L1 band) can also be observed from Fig. 4(c) and 4(d).

Fig. 5 shows the measured and simulated ARs in the boresight direction ($\theta = 0°$). With reference to the figure, the measured and simulated 3-dB AR bandwidths of L2 band are 13.0% (1.15–1.31 GHz) and 20.4% (1.10–1.35 GHz), respectively. For L1 band, the measured and simulated AR

bandwidths are given by 30.2% (1.35–1.83 GHz) and 23.2% (1.41–1.78 GHz), respectively. Both the measured and simulated VSWR and AR bandwidths entirely cover L1 and L2 bands.

Fig. 6 shows the measured and simulated radiation patterns of the dual-band CP antenna. With reference to the figure, for the entire upper hemisphere, the measured L2- and L1-band cross-polar fields are about 30 dB and 20 dB weaker than their co-polar counterparts, respectively, leading to very wide 3-dB AR beamwidths. The measured *xoz*-and *yoz*-plane half-power beamwidths (HPBWs) of L2 band are as wide as 111° and 114°, respectively. For the L1 band, the *xoz*- and *yoz*-plane HPBWs are 103° and 109°, respectively.

Fig. 7 shows the measured and simulated AR beamwidths of the antenna, with acceptable agreement between the measurement and simulation. With reference to Fig. 7(a), very wide measured L2-band 3-dB AR beamwidths of 211° and 228° are obtained in the *xoz* and *yoz* planes, respectively. For the L1 band (Fig. 7(b)), the measured 3-dB AR beamwidths in the *xoz* and *yoz* planes are 202° and 213°, respectively. Both the measured and simulated results can fully cover the upper hemisphere.

To study the effect of the corrugation, the AR beamwidths of two cavity-backed dual-band CP antennas with and without the corrugation were simulated. Fig. 8 shows the results. For brevity, it shows the results in the *xoz*($\phi = 0°$) plane only. With reference to the figure, when there are no corrugations, the AR beamwidths of the antenna are 171° and 151° at 1.227 GHz and 1.575 GHz, respectively. By inserting the corrugation, they are broadened to the respective values of 228° and 225°, fully covering the upper hemisphere. It was found that for a given corrugation depth, the AR beamwidth is affected over a narrow frequency range only. To broaden the AR beamwidth for both frequency bands, a non-uniform corrugation with different depths is therefore deployed in our design.

Fig. 9 shows the measured and simulated realized antenna gains (mismatch included) in the boresight direction ($\theta = 0°$). Again, the measured and simulated results are in reasonable agreement. With reference to the figure, both the measured and simulated results show two peaks at around 1.227 GHz (L2 band) and 1.575 GHz (L1 band). At 1.227 GHz, the measured and simulated peak values are 4.39 dBic and 5.88 dBic, respectively. The discrepancy can be expected because of imperfections in the experiment. Similar measured and simulated gains of 5.06 dBic and 5.45 dBic are obtained at 1.575 GHz (L1 band).

Fig. 10 shows the measured total antenna efficiency (mismatch included). As can be observed from the figure, the efficiency also exhibits two peaks in L1 and L2 bands, as expected. Its peak values are 82.6% and 89.3% at 1.220 and 1.550 GHz, respectively, which are very close to the L2- and L1-band frequencies. Table 2 compares our design with some previous dual-band CP antennas. With reference to the table, although the HPBW in [10] is wider than that of our design, its peak gain (< 1 dBic) and AR beamwidth (∼100°) of [10] are much smaller than those of our antenna (peak gain > 4 dBic; AR beamwidth > 200°) for both frequency bands. That design [10] has a higher profile despite its footprint

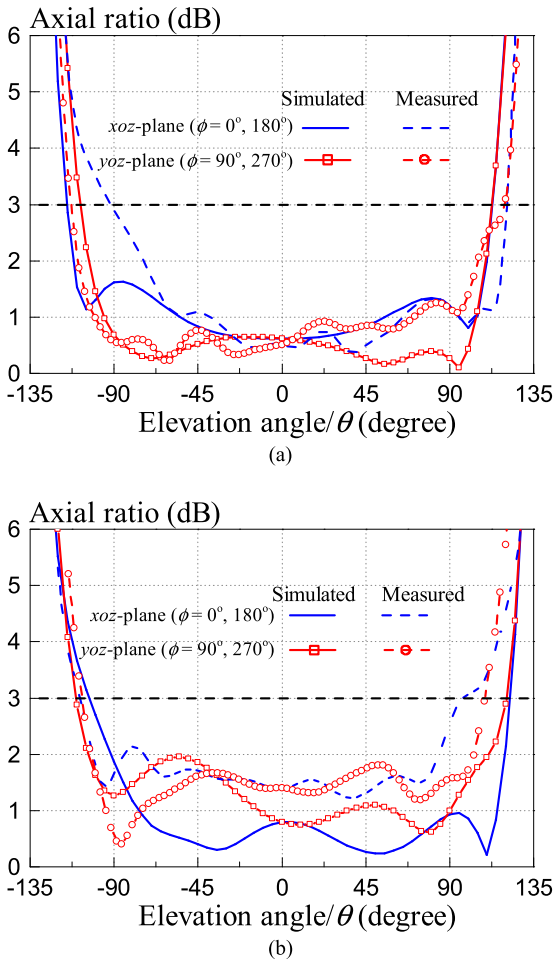

FIGURE 7. Measured and simulated AR beamwidths of dual-band CP antenna in *xoz* ($\varphi = 0°$) and *yoz* ($\varphi = 90°$) planes. (a) L2 band (1.227 GHz). (b) L1 band (1.575 GHz).

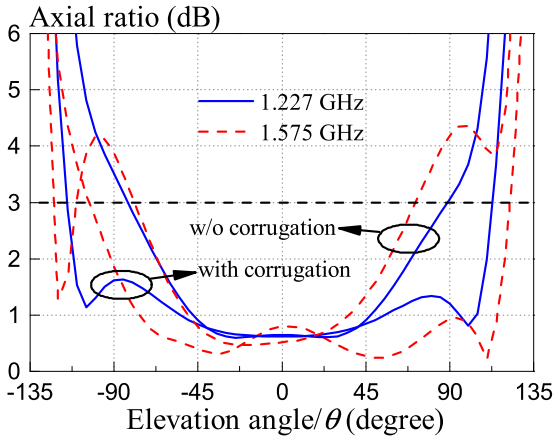

FIGURE 8. Simulated AR beamwidths of cavity-backed dual-band CP antennas with and without the corrugation at 1.227 GHz and 1.575 GHz in *xoz* ($\varphi = 0°$) plane.

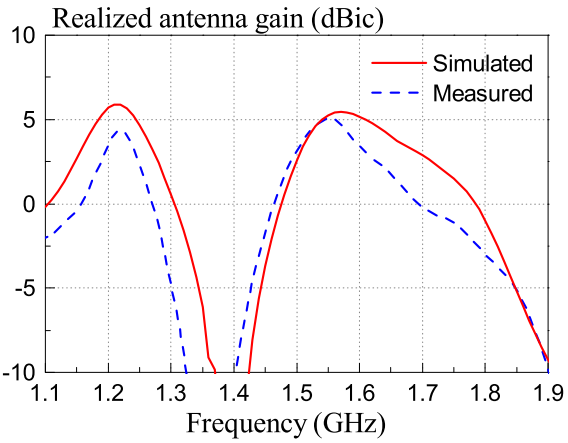

FIGURE 9. Measured and simulated antenna gains of dual-band CP antenna in boresight direction ($\theta = 0°$).

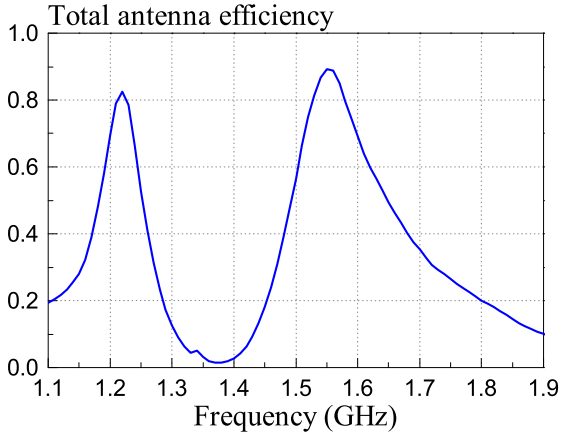

FIGURE 10. Measured antenna efficiency of dual-band CP antenna.

is smaller. Also, it vertically puts two individual quadrifilar helix antennas together to obtain the two frequency bands, requiring two feeding ports. For the design in [17], a very low profile and relatively higher peak gains can be obtained, but both its HPBW and AR beamwidth are much narrower than those of our design. It can be seen from the table that our design has wide AR beamwidths that can cover the upper hemisphere for both frequency bands. Our design can be used in GPS ground terminals, vehicles, and ships.

IV. CONCLUSION

The dual-band CP cross-dipole antenna for GPS L1- and L2-band applications has been investigated. Two sets of curved dipoles have been designed to obtain the dual-band operation; the shorter and longer arms are responsible for L1 and L2 bands, respectively. Apart from using curve dipole arms, a non-uniform corrugated cavity has been deployed to broaden the beamwidth. It has been found that the impedance and AR passbands of the dual-band antenna are sufficient for the two bands. It has been also found that the L1- and L2-band AR beamwidths are both over 200° in the two principal radiation planes, covering the entire upper hemisphere.

ACKNOWLEDGMENT

The authors would like to thank the Associate Editor and the reviewers for their useful comments.

REFERENCES

[1] B. W. Parkinson and J. J. Spilker, *Global Positioning System: Theory & Applications*, vol. 1. Washington, DC, USA: AIAA, 1996.

[2] B. R. Rao, W. Kunysz, R. Fante, and K. McDonald, Eds., *GPS/GNSS Antennas*. Norwood, MA, USA: Artech House, 2011.

[3] D. M. Pozar and S. M. Duffy, "A dual-band circularly polarized aperture-coupled stacked microstrip antenna for global positioning satellite," *IEEE Trans. Antennas Propag.*, vol. 45, no. 11, pp. 1618–1625, Nov. 1997.

[4] Q. Liu, Y. Liu, Y. Wu, M. Su, and J. Shen, "Compact wideband circularly polarized patch antenna for CNSS applications," *IEEE Antennas Wireless Propag. Lett.*, vol. 12, pp. 1280–1283, 2013.

[5] J. J. H. Wang, "Antennas for global navigation satellite system (GNSS)," *Proc. IEEE*, vol. 100, no. 7, pp. 2349–2355, Jul. 2012.

[6] C. C. Kilgus, "Shaped-conical radiation pattern performance of the backfire quadrifilar helix," *IEEE Trans. Antennas Propag.*, vol. AP-23, no. 3, pp. 392–397, May 1975.

[7] J. Tranquilla and S. Best, "A study of the quadrifilar helix antenna for global positioning system (GPS) applications," *IEEE Trans. Antennas Propag.*, vol. 38, no. 10, pp. 1545–1550, Oct. 1990.

[8] Y.-S. Wang and S.-J. Chung, "A miniature quadrifilar helix antenna for global positioning satellite reception," *IEEE Trans. Antennas Propag.*, vol. 57, no. 12, pp. 3476–3481, Dec. 2009.

[9] M. Caillet, M. Clenet, A. Sharaiha, and Y. M. M. Antar, "A broadband folded printed quadrifilar helical antenna employing a novel compact planar feeding circuit," *IEEE Trans. Antennas Propag.*, vol. 58, no. 7, pp. 2203–2209, Jul. 2010.

[10] Q.-X. Chu, W. Lin, W.-X. Lin, and Z.-K. Pan, "Assembled dual-band broadband quadrifilar helix antennas with compact power divider networks for CNSS application," *IEEE Trans. Antennas Propag.*, vol. 61, no. 2, pp. 516–523, Feb. 2013.

[11] X. Bai, J. Tang, X. Liang, J. Geng, and R. Jin, "Compact design of triple-band circularly polarized quadrifilar helix antennas," *IEEE Antennas Wireless Propag. Lett.*, vol. 13, pp. 380–383, 2014.

[12] Y. He, W. He, and H. Wong, "A wideband circularly polarized cross-dipole antenna," *IEEE Antennas Wireless Propag. Lett.*, vol. 13, pp. 67–70, Jan. 2014.

[13] R. Xu, J.-Y. Li, and W. Kun, "A broadband circularly polarized crossed-dipole antenna," *IEEE Trans. Antennas Propag.*, vol. 64, no. 10, pp. 4509–4513, Oct. 2016.

[14] D. Feng, H. Zhai, L. Xi, S. Yang, K. Zhang, and D. Yang, "A broadband low-profile circular-polarized antenna on an AMC reflector," *IEEE Antennas Wireless Propag. Lett.*, vol. 16, pp. 2840–2843, 2017.

[15] Y. M. Pan, W. J. Yang, S. Y. Zheng, and P. F. Hu, "Design of wideband circularly polarized antenna using coupled rotated vertical metallic plates," *IEEE Trans. Antennas Propag.*, vol. 66, no. 1, pp. 42–49, Jan. 2018.

[16] W. J. Yang, Y. M. Pan, and S. Y. Zheng, "A low-profile wideband circularly polarized crossed-dipole antenna with wide axial-ratio and gain beamwidths," *IEEE Trans. Antennas Propag.*, vol. 66, no. 7, pp. 3346–3353, Jul. 2018.

[17] S. X. Ta and I. Park, "Dual-band low-profile crossed asymmetric dipole antenna on dual-band AMC surface," *IEEE Antennas Wireless Propag. Lett.*, vol. 13, pp. 587–590, 2014.

[18] S. X. Ta, I. Park, and R. W. Ziolkowski, "Circularly polarized crossed dipole on an HIS for 2.4/5.2/5.8-GHz WLAN applications," *IEEE Antennas Wireless Propag. Lett.*, vol. 12, pp. 1464–1467, 2013.

[19] S. X. Ta, H. Choo, I. Park, and R. W. Ziolkowski, "Multi-band, wide-beam, circularly polarized, crossed, asymmetrically barbed dipole antennas for GPS applications," *IEEE Trans. Antennas Propag.*, vol. 61, no. 11, pp. 5771–5775, Nov. 2013.

[20] W. S. Yeoh, K. L. Wong, and W. S. T. Rowe, "Wideband miniaturized half bowtie printed dipole antenna with integrated balun for wireless applications," *IEEE Trans. Antennas Propag.*, vol. 59, no. 1, pp. 339–342, Jan. 2011.

[21] J. Yeo and J.-I. Lee, "Modified series-fed two-dipole-array antenna with reduced size," *IEEE Antennas Wireless Propag. Lett.*, vol. 12, pp. 219–222, 2013.

[22] Y.-X. Sun, K. W. Leung, and K. Lu, "Broadbeam cross-dipole antenna for GPS applications," *IEEE Trans. Antennas Propag.*, vol. 65, no. 10, pp. 5605–5610, Oct. 2017.
[23] M.-S. Wang, X.-Q. Zhu, Y.-X. Guo, and W. Wu, "Compact circularly polarized patch antenna with wide axial-ratio beamwidth," *IEEE Antennas Wireless Propag. Lett.*, vol. 17, no. 4, pp. 714–718, Apr. 2018.
[24] C. Deng, Y. Li, Z. Zhang, and Z. Feng, "A circularly polarized pattern diversity antenna for hemispherical coverage," *IEEE Trans. Antennas Propag.*, vol. 62, no. 10, pp. 5365–5369, Oct. 2014.
[25] N. Marchand, "Transmission line conversion transformers," *Electronics*, vol. 17, pp. 142–145, Dec. 1944.
[26] Y.-H. Chun and J.-S. Hong, "Compact wide-band branch-line hybrids," *IEEE Trans. Microw. Theory Techn.*, vol. 54, no. 2, pp. 704–709, Feb. 2006.

YU-XIANG SUN was born in Yingcheng, China, in 1987. He received the B.Eng. degree in electronic information science & technology and the M.Sc. degree in radio physics from Wuhan University, Wuhan, China, in 2010 and 2012, respectively, and the Ph.D. degree in electronic engineering from the City University of Hong Kong, Hong Kong, in 2016.

From 2012 to 2013, he was a Research Assistant with the Department of Electronic Engineering, City University of Hong Kong, where he has been a Post-Doctoral Fellow since 2016.

Dr. Sun serves as a Technical Reviewer for the IEEE TRANSACTIONS ON ANTENNAS AND PROPAGATION, the IEEE ANTENNAS AND WIRELESS PROPAGATION LETTERS, SENSORS, and *IET Microwaves, Antennas and Propagation*. His current research interests include dielectric resonator antennas (DRA), GPS antennas, and millimeter-wave antennas.

KWOK WA LEUNG (S'90–M'93–SM'02–F'11) was born in Hong Kong. He received the B.Sc. degree in electronics and the Ph.D. degree in electronics engineering from the Chinese University of Hong Kong, Hong Kong, in 1990 and 1993, respectively. In 1994, he joined the Department of Electronic Engineering (EE), City University of Hong Kong (CityU), where he is currently a Chair Professor and the Associate Head of the EE Department. In 2006, he was a Visiting Professor at the Department of Electrical Engineering, The Pennsylvania State University , State College, PA, USA. His research interests include antenna designs, guided wave theory, computational electromagnetics, and mobile communications.

Prof. Leung received the International Union of Radio Science (USRI) Young Scientists Awards in Japan and Russia, in 1993 and 1995, respectively. He also received the CityU Research Excellence Award in 2013, and the Departmental Outstanding Teacher Awards in 2005, 2010, and 2011, respectively. He also received the highly prestigious First Class Award (Natural Science) in the 2016 Higher Education Outstanding Scientific Research Output Awards (Science and Technology) of the Ministry of Education, China. His students received the 2015 iWEM Student Best Paper Award, the 2015 IEEE AP-S Eugene F. Knott Memorial Pre-Doctoral Research Award, and the 2014 IEEE MTT-S Undergraduate/Pre-graduate Scholarship. He was the Chair of the IEEE AP/MTT Hong Kong Joint Chapter for 2006 and 2007. He was the Technical Program Chair, the 2008 Asia-Pacific Microwave Conference, Hong Kong, the Technical Program Co-Chair, the 2006 IEEE TENCON, Hong Kong. He was the Guest Editor of *IET Microwaves, Antennas and Propagation*. He served as an Associate Editor for the IEEE ANTENNAS AND WIRELESS PROPAGATION LETTERS. He was also an Associate Editor for the IEEE TRANSACTIONS ON ANTENNAS AND PROPAGATION and received Transactions Commendation Certificates twice in 2009 and 2010 for his exceptional performance. He was the Editor-in-Chief of the Transactions from 2013 to 2016. He was a Distinguished Lecturer of the IEEE Antennas and Propagation Society.

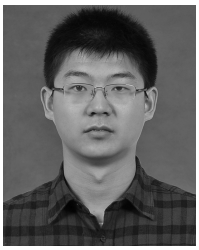

JIAN REN was born in Dezhou, China, in 1989. He received the B.Sc. in electronic engineering and the M.Eng. degree in electromagnetics and microwave technology from Xidian University, Xi'an, China, in 2012 and 2014, respectively. He is currently pursuing the Ph.D. degree with the City University of Hong Kong, Hong Kong.

In 2015, he was a Research Assistant at the City University of Hong Kong. His research interests include microwave circuits, metamaterials, RFID, and dielectric resonator antennas.